

Thermal comfort modeling in transient conditions using real-time local body temperature extraction with a thermographic camera

Andrei Claudiu Cosma and Rahul Simha

Department of Computer Science, School of Engineering and Applied Science, The George Washington University, USA

Abstract

This work evaluated the use of thermographic cameras as a non-invasive method to automatically model human thermal comfort in transient conditions, using data from 30 healthy subjects tested in an office setup with ambient temperatures between 21.11°C and 27.78°C . Office temperature, relative humidity, exposed skin temperature and clothing temperature were automatically measured over approximately 27 minutes per subject, using remote sensors and avoiding any contact with the subjects. Thermal comfort levels were evaluated using subjects' feedback, recorded every minute for the entire experiment. Clothing insulation and metabolic rate were kept relatively constant for this experiment (0.54 clo and 1.1 met). Average skin temperature was extracted from five different locations, with average temperatures of 33.5°C , 34.5°C , and 35.6°C corresponding to cold discomfort, comfort and warm discomfort respectively. Average clothing temperature was also extracted from three different location, with 32.3°C , 33.8°C and 35.0°C corresponding to the same three comfort levels. Relative humidity levels were similar for all subjects, with average values between 38% and 33%. Results showed significant correlation between observed skin temperature, clothing temperature and thermal comfort level. Also, collected data showed that the temperature difference between different body locations was highly correlated with thermal comfort, and the variance of skin temperature over a small area was significantly correlated with thermal comfort. The results suggest that non-invasive thermographic cameras that combine visual and thermal modes are sufficiently accurate in real-world settings to drive control of HVAC systems.

Keywords: thermal comfort, thermoregulation system, thermographic camera, skin temperature, building automation

1 Introduction

The increased demand for energy efficient buildings to reduce greenhouse gas emissions has pushed engineers to identify and address the issues with the main source of energy consumption within office and residential buildings. Based on the most recent CBECS [1] and RECS [2] reports, energy usage for residential and commercial buildings in the US represents 40% of the total energy used throughout the country. The same reports revealed that almost 50% of total energy used in homes and 33% of total energy used in commercial

buildings came from heating, ventilation and air conditioning (HVAC) systems. That is a significant amount of energy consumed on a daily basis simply to provide physical comfort, and for which any possible reduction can have a significant impact on the total amount of energy used.

Traditionally, HVAC systems work on a setpoint temperature computed using attributes of the environment where they act (such as air temperature and air humidity) and other constants determined based on large scale experiments (such as clothing insulation and metabolic rate). This approach was developed by Fanger in the 1970s [3] and later it was refined in the ASHREA-55 standards. These models sought to ensure that a building equipped with HVAC systems is able to keep at least 80% of its occupants comfortable. However, a study of 215 office buildings in US, Canada, and Finland [4] showed that only 11% of the studied buildings had at least 80% of the occupants comfortable. Improper calculation of the setpoint temperature typically resulted in energy waste. Similar results were found by other studies [5, 6, 7].

Also, it was shown that attributes which were considered constant by the traditional model can change over time and can affect individual thermal comfort (such as clothing insulation, metabolic rate or age). For this reason, recent work in the literature has focused on developing HVAC control systems that add the occupants of the space into the control loop. This has been done in three ways: using occupants' feedback to adjust the set point temperature, using personal comfort systems for individualized comfort, or modeling individual thermal comfort. Setpoint adjustments based on user feedback were investigated in [8, 9, 10] by allowing the user to control the temperature through a local thermostat or by offering them an online system to provide feedback in real time. Advantages and possible issues with this approach were analyzed in [11]. Their results showed that there was a significant gap between users expectations from the local temperature controller and the system designers perspective on the users needs.

The second approach for individual thermal comfort employed personal comfort systems (PCS), designed to keep occupants comfortable within their personal space. This approach proposed an energy efficient system by moving the focus from keeping the space within a set point temperature, to keeping smaller space enclosures within the set point temperatures. A few ideas were based on retrofitting office furniture, such as chairs [12] or desks [13], to integrate cooling and heating elements. Others focused on directing the air towards the occupant's location [14].

However, these first two approaches have a few limitations: they depend on user feedback, the user is required to physically interact with the system to achieve their desired results (such as turning a switch), and the user feedback is connected to a precise location, which is inapplicable if the user moves within the building (for example, to a conference room). For these reasons, a third approach was explored, which uses a mathematical modeling of thermal comfort based on physiological information extracted directly from individual occupants of the building. An in depth literature reviewed on thermal comfort modeling presented by Rupp et al. [15] showed significant growth of papers in this area. A large number of these studies (such as [16] and [17]) have focused on using existing datasets and machine learning algorithms to propose a better thermal comfort model than Fanger's PMV model using the same data as input. Some researchers, such as Liu et al. [18], focused on modeling thermal comfort using heart rate variability. Their results indicated that sympathetic activity was highly correlated with thermal discomfort, and the ratio between low and high frequency (LF/HF) components of heart rate variability (HRV) may be used as an indicator of thermal comfort. Other researchers have focused on extracting skin temperature, using sensors attached to the subject's body, to model thermal comfort based on human body thermoregulation [19, 7, 20, 21]. Moreover, Chaudhuri et al. [22] showed that using normalized hand skin temperature based on inter-individual differences (such as clothing insulation and body surface area), the thermal sensation can be more accurately predicted. Similar results were found by Choi et al. in [23], which showed that body mass index(BMI) affects the temperature dynamics and that wrist temperature was the most significant body segment for assessing thermal sensation. Finally, Ghahramani et al. [24] collected skin temperature using eyeglasses outfitted with point IR sensors to monitor individual's thermoregulation. All these works showed that thermal comfort or sensation was correlated with thermoregulation, and that skin temperature can be used to model thermal comfort. Multiple body parts were identified as target points for thermal comfort modeling, but a few of them were highly sensitive to thermal comfort, such as wrist, head and chest.

A few more recent works focused on using thermographic cameras as a means to model thermal comfort. These cameras have the advantage of not requiring physical contact with the subjects while measuring their skin temperature. Preliminary studies focused on manual measurements of face temperature using hand-held thermographic cameras. Burzo et al. [25] used average facial temperature and other physiological signals to

predict subject’s level of discomfort without any explicit input from the user. Pavlin et al. [26] evaluated multiple forehead key-points as a measure of thermal comfort. Finally, Ranjan et al. [27] included head and hand temperatures manually extracted from a thermographic camera to model the thermal needs of the space occupants. All these works showed that average face temperature computed using thermographic cameras was highly correlated to thermal comfort, and that it can be used to predict the thermal needs of the building occupants.

Based on the results of these preliminary studies and the recent development of low-cost consumer grade thermographic cameras, we believe that these sensors are a promising technology to help solve the thermal modeling problem in a non-invasive way. While the above studies are based on hand-held cameras with explicit manual pointing for optimal measurement, we study the potential of a wall-mounted camera in a real office setting where the subject moves around and body parts are obscured or come in and out of the field of view, and where identification of thermal comfort is performed in real-time. The proposed sensing platform combines an inexpensive thermographic camera with a color-distance sensor to automatically localize measurements. Furthermore, we examine whether clothing temperature and identification of temperature differences amongst body parts can lead to more accurate assessment of thermal comfort. Finally, a comprehensive study with 30 healthy subjects was conducted to examine whether thermal comfort has a different signature from warm and cold discomfort in transient conditions.

2 Method

To test our proposed system capabilities to model thermal comfort levels, we designed an experiment based on an office setup with transient conditions, where we varied the office temperature and queried the thermal comfort of the occupants. Our proposed sensing platform was used to collect the thermal profiles of the following body parts: hand, elbow, shoulder, chest and head, including left or right. These body parts were identified as highly relevant for thermal comfort modeling by [21, 23, 22]. A feedback form was used to collect thermal comfort information from subjects. We describe in detail the proposed experiment in Section 2.1.

Our proposed non-invasive technology to automatically model thermal comfort combines three sensors, a thermographic camera, a depth sensor and a color camera, to create an augmented representation of the world, which we called RGB-DT (RedGreenBlue-DepthTemperature). This new world representation was used by our algorithms to detect and track humans within the environment, and to identify different human body parts for which the thermal profile was computed. This system is described in detail in Section 2.2.

Finally, all data collected by the sensing platform and subjects’ feedback forms were used to analyze the interaction between genders, Thermal Comfort Vote (TCV) levels and body parts temperatures. The purpose of this analysis was two fold: verify if there is a difference in skin and clothing temperature response between males and females at different TCV levels, and validate the use of skin and clothing temperature as a mean of thermal comfort modeling. Complete data analysis can be found in Section 3.

2.1 Experimental Design

2.1.1 Subjects

30 healthy volunteers participated in this study (15 females and 15 males), primarily undergraduate and graduate students at The George Washington University. Their age ranged between 20 and 42 years old. Every subject was asked to wear a similar outfit (such as pants, t-shirt and regular shoes) and was instructed on how to self-report their clothing insulation using the garment insulation table from [28]. Data from the 30 subjects showed that the average clothing insulation was 0.44 clo with $SD = 0.07$ clo. After we considered the added insulation when sitting on a chair (+0.1 clo for standard office chair), the final average clothing insulation was 0.54 clo. Metabolic rate was constant during the experiment, around 1-1.1 met, equivalent to sedentary office activity. All demographic measurements were recorded in a questionnaire at the beginning of the experiment and are presented in Table 1.

Table 1: Demographic information.

Variable	Mean	SD	Min	Max
Age	26	5.8	20	42
Height(cm)	172.2	9.9	155	196
Weight(kg)	73.1	17.4	48	120

2.1.2 Office setup

The experiment took place in an office room at The George Washington University. The room was located in the middle of the School of Engineering and Applied Science building, and it had no windows or exterior walls. The office was disconnected from the central HVAC unit, such that the heating and cooling was controlled locally through portable space heaters and an air conditioner. For this experiment, two radiant heaters were used together with an 14,000 BTU portable air conditioner. The office furniture consisted of a desk and a chair, placed on a side of the room. The sensing platform, the heaters and air conditioner were placed on the other side of the room. The room layout can be seen in Figure 1.

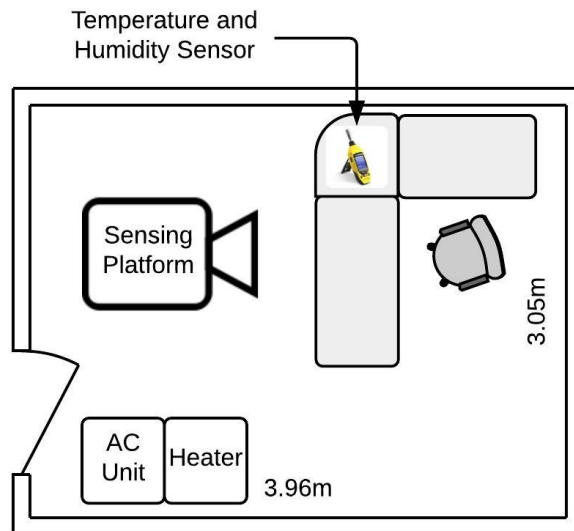


Figure 1: Office layout.

Indoor conditions were monitored by measuring the air temperature and relative humidity in the immediate vicinity of the subject. These measurements were not used directly by the proposed algorithms, but they were measured to ensure that the indoor conditions were consistent across all subjects' recordings. Finally, the air flow was less than 0.2 m/s, as recommended by ASHRAE-55 [28].

2.1.3 Experimental procedures

The experiment took around 40 minutes for each subject. This duration included subject acclimatization (standby time), answering a short survey, and data acquisition. Most thermal comfort experiments include an acclimatization period, such that subjects achieve a target metabolic rate and thermal condition, usually affected by previous activities and environments. Some works in this area used a different environment for acclimatization [19, 25, 26], while others used the experimental environment for acclimatization and data collection [7, 18, 27]. We followed the later one, since we wanted to eliminate subjects' reaction to the initial state of the environment and to start the experiment from a stable thermal condition with respect

to the experimental environment. Subjects were asked not to exercise one hour before the data collection appointment, for a rapid skin temperature stabilization. The recommended acclimatization time in the literature is around 30 minutes. Since we did not test extreme conditions (really high or low temperatures), and the temperature jump for all subjects was lower than 3°C, an acclimatization period between 10 and 20 minutes was selected to ensure that the skin temperature reached a stable condition.

During the acclimatization, each subject had to answer a short survey regarding demographic information, after which he/she was instructed on how to answer the feedback form questions during the experiment. The feedback questions were with respect to the TCV and thermal sensation vote (TSV), and they had to be answered every minute during the experiment. A timer was set to audibly alert the subjects when they had to answer the feedback questions.

An office building indoor environmental quality study from 2008 [29] determined that the typical minimum and maximum temperatures for an office building were 19.4°C to 27.8°C. Also, these temperatures were labeled by subjects as “cool” and “warm” in a chamber study [19]. Based on these observations, we selected the temperature range for our experiment to be 21.11°C to 27.78°C. For each subject, the room temperature was set to 21.11°C before the acclimatization, and kept constant till the beginning of the recording. During the experiment, the room was heated at approximately 0.24°C per minute for 27 minutes, from 21.11°C to 27.78°C. Although the temperature changes are not exactly controlled in a fine-grained manner, we observed that similar conditions were tested in day 4 of the experiment used in [24]. These conditions were faster than normal transient conditions, and the main purpose was to amplify the thermoregulation response in a shorter amount of time. The accelerated schedule of temperature change allowed for efficient evaluation, but it fairly raises the question of how a model based on accelerated transient conditions can be applied to other, perhaps more gradual, transient conditions. The same methodology would apply, and the apparatus would likely be the same, in which case further testing under multiple transients could lead to an adjusted model that includes measures of transient rates.

2.1.4 Measurements

Two types of measurements were collected during the experiment:

- environmental conditions: room temperature and relative humidity were collected every minute, using a measurement device placed in the vicinity of the subject (see Figure 1);
- subject’s thermal profile: skin and clothing temperature were recorded continuously for the entire experiment at 9 frames per second, using the proposed sensing platform. This was placed such that it faced the subject (see Figure 1);

In contrast with existing methods, clothing temperature was also considered in modeling thermal comfort. The clothing temperature is driven by two main factors: clothing insulation level and heat transfer between the environment and skin surface. Similar to the skin temperature literature where the heat transfer is analyzed to model thermal comfort, constant clothing insulation level was assumed to model the heat transfer through clothing. We focused on the chest and shoulders because these were identified as important locations to model comfort, and they are typically covered by clothing.

2.1.5 Subject Feedback

For thermal comfort assessment, each subject had to provide the thermal comfort vote (TCV) every minute for the entire experiment. The vote was recorded based on a modified Bedford scale [30]. Originally, the Bedford scale consists of seven levels: much too warm (+3), too warm (+2), comfortably warm (+1), comfortable (0), comfortably cool (-1), too cool (-2), and much too cool (-3). However, since we were interested in distinguishing comfort from discomfort (warm or cold), we combined scales +1, 0 and -1 in only one as comfort. Thus, our modified TCV scale has 5 levels: high warm discomfort (+2), warm discomfort (+1), comfortable (0), cold discomfort (-1), and high cold discomfort (-2).

Thermal sensation vote (TSV) was also collected every minute during the experiment. The TSV scale was based on 7 levels ASHRAE Standard-55 [28]: cold (-3), cool (-2), slightly cool (-1), neutral (0), slightly warm (+1), warm (+2), and hot (+3).

2.2 Sensing Platform

The sensing platform design was governed by the following principles: low cost sensors, small form-factor device and real time capabilities. The data acquisition and processing pipeline of the system are described in Section 2.2.1, and 2.2.2 respectively, with an overview of the entire system architecture shown in Figure 2.

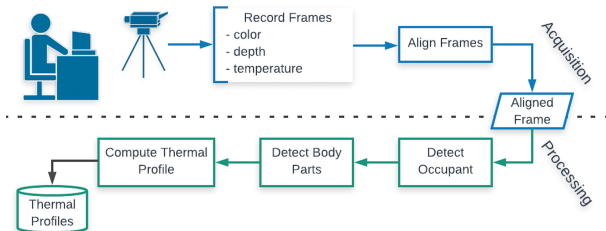


Figure 2: Sensing platform architecture.

2.2.1 Data Acquisition

Our proposed sensor fusion was designed using off-the-shelf sensors. The total system cost was around \$300. The hardware components are (see Figure 3 for a picture of the system):

- a depth sensor and color camera combination (Kinect 2), to identify and track office space occupants;
- a thermographic camera (Flir Lepton) with thermal sensitivity of $0.05\text{ }^{\circ}\text{C}$, to capture the temperature information of the occupants;
- a point IR sensor (MLX90614) with thermal sensitivity of $0.02\text{ }^{\circ}\text{C}$, to calibrate the thermographic camera;

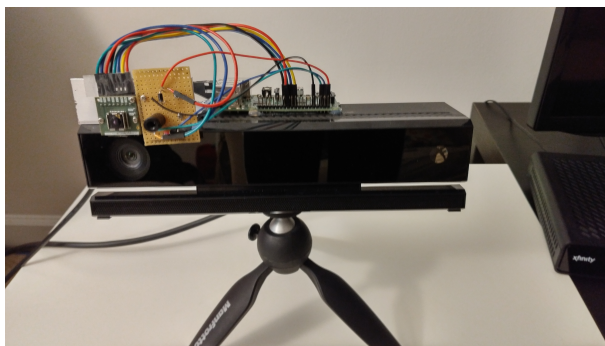


Figure 3: Sensing platform hardware.

All data was acquired in real time and sent to the software modules for processing. Since different sensors have different frame rates, the slowest sensor set the sensing platform speed. In our case, the sensing platform speed was around 9 frames per second, which was the maximum speed of the thermographic camera. We also needed to account for the different image resolutions of each sensor: for example, the thermographic camera uses an 80×60 resolution, while the depth camera uses 640×480 , and the color camera uses 1920×1080 . In this case, we decided that the best resolution was the depth camera resolution, because the image registration process used the depth camera image plane as the reference plane.

2.2.2 Data Processing

The end goal of our sensing platform was to describe the thermal profile of the identified human body parts, whose differences have the potential for improving thermal comfort prediction. Based on recent work in the field, such as [7, 19, 20, 21], and considering the constraints of our remote sensing platform that can see mainly upper body (considering the office setup), we identified the following body parts to be of interest for our experiment: hands, elbows, shoulders, chest and head. We considered using neck information too, but initial experiments showed that this was occluded by the head most of the time, due to the camera placement (higher than the occupant’s head).

To accurately identify, track and compute thermal profile of these body parts, we proposed a new augmented world representation, which we call RGB-DT. This new representation combines three types of information: color (Red-Green-Blue), spatial (Depth) and thermal (Temperature). Our software aligned these information channels, such that each object in the field of view of the camera can be described by its color, 3D location and surface temperature. The proposed model can be seen in Figure 4.

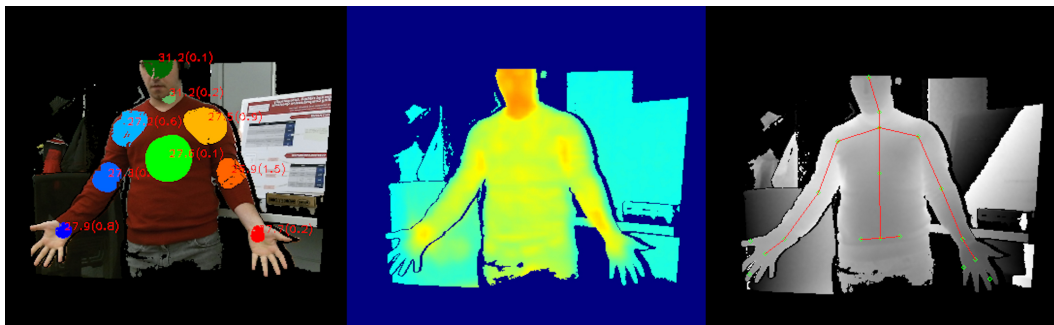


Figure 4: RGB-DT model, from left to right: color information with overlapped detected body parts, thermal information and depth information with overlapped detected joints.

We used depth and color information from a Kinect 2 sensor to first detect the occupant. Then, the occupant’s joints were identified through an algorithm provided along with the Kinect 2 sensor. Using the identified joints, we computed the 3D location of each body part, by using the fact that all of them either overlapped with a joint (such as wrists), or could be derived from their position in relation to a known joint (such as the chest, situated between and below the shoulder joints). We observed that temperature readings coming from a single point were significantly affected by noise in data and processing errors, such as noise from thermal image upscaling, inaccuracy in body part location or occlusions. To eliminate the temperature noise issues, we computed a local area around each body part location, which we called a patch, and we extracted the average temperature information over this area, instead of a single point measurement. The computed patch ensured that all points within the patch came from the same surface and were points of the same body part. Finally, we used thermal information from the RGB-DT values and computed patches to extract the thermal profile of each body part. Each thermal profile consisted of the average temperature of the patch around the detected part and the variance of the patch temperature (see Figure 4).

3 Data analysis

For the experiment, the data collection phase took 4 weeks and resulted in 15 hours of video and 5TB of RGB-DT data. User feedback was automatically logged using digital survey tools. The two streams of data were automatically synchronized using associated timestamps and analyzed using R (for statistical analysis).

Before subjects entered the room, the temperature was set and kept at 21.11°C. During the experiment, the room was heated up to 27.78°C. The average room temperature measurements for all subjects and the associated standard errors are displayed in Figure 5a. Relative humidity for the office space was also measured for the entire experiment. On average, the relative humidity was 36% (with SE = 6%). However,

as Figure 5b shows, there was a common variation of humidity across all subjects. The room heater dried the air 6% on average.

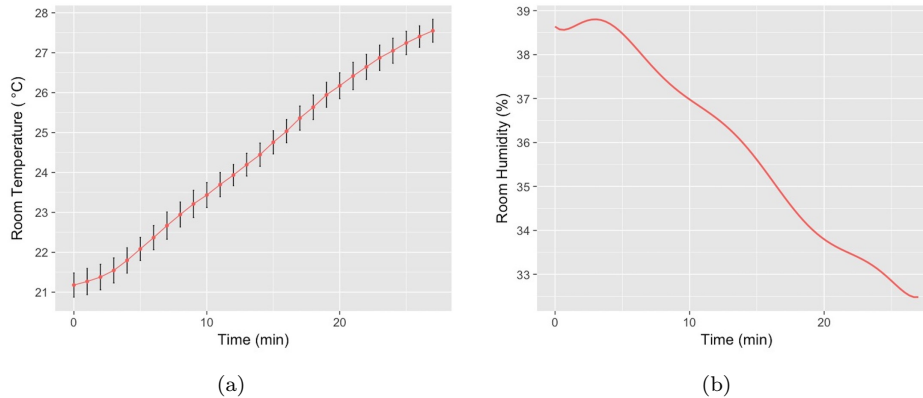


Figure 5: Average room temperature and relative humidity during the experiment.

Initial review of the data revealed that all 30 subjects experienced comfort, but only 13 experienced cold discomfort and 22 warm discomfort. Furthermore, six subjects were identified as not appropriate for data analysis. The main reasons for excluding these subjects are: incomplete data (due to sensors malfunctions) or zero comfort variance (subject felt comfortable for the entire temperature range). We chose to discard the data for the subjects who experienced no variance in comfort because we could assume that the generated thermal comfort model from the other subjects with more restrictive comfort profiles would also apply to subjects with a wider range of temperature comfort. The remaining 24 subjects experienced at least two different TCV levels: five of them experienced cold discomfort and comfort, eleven of them experienced comfort and warm discomfort, and eight of them experienced all three TCV levels.

Although both the TSV and TCV responses from subjects were collected, similar to [24, 27], we focused on TCV responses to directly model thermal preferences. Other researchers, such as [16, 21, 23, 22, 19], have focused on the TSV values to model preferences, and they also showed that in many situations the TCV and TSV are highly correlated. This can be also observed in our Table 2. Results showed that the neutral state (TSV=0) corresponds to thermal comfort, while slightly cold/warm sensation overlaps mostly with thermal comfort state and up to 35% with cold/warm discomfort. Finally, the cool and warm state identify with cold and respectively warm discomfort. However, there are situations where subjects are comfortable, although their sensation is outside comfort range based on the TSV value. For these reasons, we investigated the relationship between the recorded skin and clothing temperatures and the TCV.

3.1 Gender differences in thermal comfort

A summary of the average patch temperature for different thermal comfort levels is presented in Table 3, grouped by gender. It can be seen that the average temperature for all considered body parts increases with the TCV value, and most of these match between males and females. Also, body parts covered by clothes, such as torso and shoulder, have a lower patch temperature. Finally, for a TCV of -1 (cold discomfort) the skin temperature was significantly higher than the temperature of clothing patches, whereas for a TCV of 1 (warm discomfort), the gap is much smaller.

In the first test, we evaluated the impact of gender, TCV levels and their relationship to average patch temperature. The scope of this test was to check whether males and females responded differently at given TCV levels, when they were compared using individual patch temperatures. This relationship was analyzed using repeated measures Factorial ANOVA test, where the repeated measures were the three TCV levels. However, since not all subjects experienced all three TCV levels during the experiment, we repeated the analysis for two different groups: subjects that felt cold discomfort and comfort, and subjects that felt comfort and warm discomfort. Because data was collected continuously, there are multiple responses for

Table 2: TSV values and the associated percent of TCV votes.

		TCV				
		-2	-1	0	+1	+2
TSV	-3	0	0	0	0	0
	-2	0	60.9	39.1	0	0
	-1	0	20.0	80.0	0	0
	0	0	0	98.8	1.2	0
	+1	0	0	65.1	34.9	0
	+2	0	0	26.3	66.4	7.3
	+3	0	0	1.1	56.3	42.6

Table 3: Average patch temperature measurements ($^{\circ}\text{C}$) grouped by TCV and gender.

TCV	Gender	LH	LE	LS	RH	RE	RS	Head	Torso
-1	Male	32.9	34.3	32.6	32.5	33.8	32.5	34.9	31.4
	Female	32.2	33.1	32.9	32.5	34.0	32.9	35.3	31.5
0	Male	34.0	35.0	34.0	34.0	35.0	34.0	36.4	33.4
	Female	33.4	33.9	33.6	33.1	34.2	33.8	36.0	33.2
1	Male	35.2	35.6	34.9	35.0	35.8	34.9	37.0	34.8
	Female	35.4	35.1	35.0	35.0	35.2	35.3	37.1	34.8

Note: LH=Left Hand, LE= Left Elbow, LS=Left Shoulder, and (RH,RE,RS) are the equivalent for the right arm.

each TCV levels for each subject. So, for each subject, the average response was computed for all available TCV levels. The F-ratio and p-value resulting from ANOVA test are reported in Table 4 and 5.

Results showed that the interaction between gender and TCV level was not significant ($p\text{-value} > .05$) for all body parts, so, we analyzed the main effects individually. When males and females were compared, results showed that if we ignore the TCV level, the gender of the subject did not influence the patch temperature ($p\text{-value} > .05$). This result was consistent for all considered body parts. For the second main effect, when comfort and discomfort (cold or warm) were compared, results showed that if we ignore the subject gender, the TCV level influenced the patch temperature ($p\text{-value} < .05$). There were a few patch temperatures (RH, RE) that did not have a significant F-value when comfort was compared with cold discomfort. However, these patches were identified as highly exposed to noise, and we reviewed in detail the source of this noise in Section 3.4. To conclude, males and females did not respond significantly differently for same TCV levels, given all selected body parts. Thus, for the remainder of this paper, both genders are treated as a single subject group. However, subjects responded significantly differently for the three TCV levels, given their skin and clothing temperature.

3.2 Principal component analysis

A principal component analysis test was run on the thermal profiles data to investigate the interaction between different body parts, to identify the main components and to eliminate possible redundant data. First, all detected body parts were used and the correlation matrix was computed. Table 6 shows the content

Table 4: Repeated measures Factorial ANOVA test for TCV (-1 and 0) and Gender interaction.

Body Part	Gender		TCV		Gender:TCV		Assumptions	
	F(1,10)	p-value	F(1,10)	p-value	F(1,10)	p-value	Normality ^a	HOV ^b
LH	0.203	0.668	6.137	0.048	0.072	0.798	✓	✓
LE	3.552	0.108	10.520	0.017	0.143	0.718	✓	✓
LS	0.155	0.707	15.929	0.007	2.181	0.190	✓	✓
RH	0.074	0.795	4.323	0.082	0.647	0.451	✓	✓
RE	0.163	0.700	2.356	0.176	1.363	0.287	✓	✓
RS	0.003	0.957	12.355	0.012	1.149	0.324	✓	✓
Head	0.004	0.949	5.835	0.052	0.740	0.422	✓	✓
Torso	0.056	0.820	13.387	0.010	0.265	0.624	✓	✓

^aNormality tested using Shapiro-Wilk Test

^bHomogeneity of variance(HOV) tested using Levene's Test

of the correlation matrix, while Figure 6 is a visual representation of the same data.

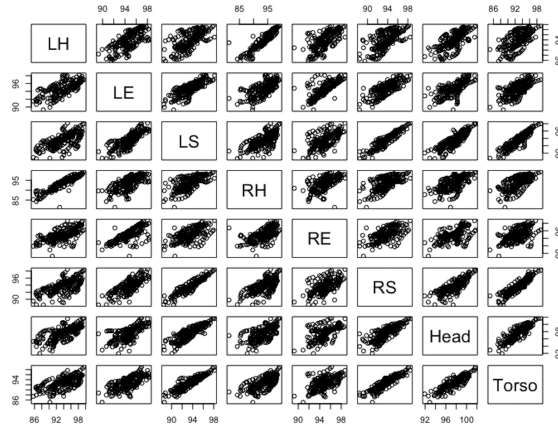


Figure 6: Correlation graphic for all body parts.

The correlation matrix shows that all body parts were significantly correlated (correlation $> .5$), but some of them were highly correlated (correlation $> .9$). Highly correlated variables were an indicator of multicollinearity in data. These results were also supported by the determinant of the correlation matrix that had a value close to 0 (4.71563e-05), and by the correlation matrix which was different from the identity matrix, based on the Bartlett Test ($p < 0.001$). We identified two groups of highly correlated values: equivalent body parts between left and right arm (e.g. LH and RH), and body parts covered by clothing items (LS, RS and Torso). These groups were also supported by the correlation graphic, and they were identified as plots that closely follow a diagonal line distribution.

The left and right arm correlation can be explained by the human body thermoregulation which is symmetric in response, as long as the temperature within the environment is uniform. In those conditions, both arms responded similarly to the changes in the environment. This symmetry was highly important for our proposed sensing platform, since it allowed the automatic system to detect at least one arm, without losing significant thermal comfort information. If both arms were detected, the temperature from both was

Table 5: Repeated measures Factorial ANOVA test for TCV (0 and +1) and gender interaction.

Body Part	Gender		TCV		Gender:TCV		Assumptions	
	F(1,16)	p-value	F(1,16)	p-value	F(1,16)	p-value	Normality ^a	HOV ^b
LH	0.124	0.730	39.709	3.94e-05	3.787	0.075	✓	✓
LE	2.758	0.123	53.199	9.56e-06	3.981	0.069	✓	✓
LS	0.017	0.899	79.617	1.21e-06	0.626	0.444	✓	✓
RH	0.360	0.560	45.339	2.09e-05	5.769	0.033	X ^c	✓
RE	4.649	0.052	50.095	1.29e-05	0.932	0.353	✓	✓
RS	0.344	0.569	150.210	3.82e-08	2.611	0.132	✓	✓
Head	0.143	0.712	23.641	0.00039	1.047	0.326	✓	✓
Torso	0.003	0.960	92.173	5.55e-07	0.014	0.907	✓	✓

^aNormality tested using Shapiro-Wilk Test

^bHomogeneity of variance(HOV) tested using Levene's Test

^cThe distribution isolating males failed the normality test.

used to improve the thermal profile of the arm.

With respect to the body parts covered by clothing, their correlation can be explained by the fact that these measurements came from neighboring areas from the upper body, and they represent measurements of the same surface (clothing). However, the temperature range for LS/RS was significantly different than the torso, because of the skin temperature behind that clothing patch. For this reason, it was important to consider torso thermal profile separately from LS/RS.

Based on the above observations, the main important body parts to track, without losing significant information, were hand (any), elbow (any), shoulder (any), torso and head. Using these body parts, we ran the principal component analysis test. The correlation matrix remains the same, without the rows and the columns associated with the discarded body parts (for this experiment, the right arm was randomly selected to be discarded from the data). The new matrix passed the multicollinearity test, with the determinant value (0.0072) significantly higher than the accepted threshold (0.00001). The Kaiser-Meyer-Olkin measure verified the sampling adequacy for the analysis, with the overall KMO=0.83, and all KMO values for individual body parts were > 0.79 , which is well above the acceptable limit of 0.5. Bartlett's test of sphericity, $\chi^2(10) = 1014.86, p < 0.001$, indicated that correlations between body parts were sufficiently large for PCA.

An initial analysis was run with the maximum number of components, five components in our case, to obtain the eigenvalues for each component. From the five components, only one had the eigenvalue higher than Kaiser's criterion of 1 and it explained 79% of the variance. This result was validated by the inflexion point on the screen plot. So, one component was retained for the final analysis. Table 7 shows the factor loadings (PC1), commonalities (h^2), and the unexplained variance (u^2).

Based on these results, we can conclude that the selected body parts were members of the same component, and this component represents the thermal response of a subject to the environmental conditions.

3.3 Derived measurements

As shown in Section 3.1, the skin patches had higher temperature than the clothing ones. However, it was observed that the temperature difference between skin and clothing patches decreases with an increase in TCV level. This phenomenon can also be observed in Figure 7a. On the left side of the graphic, corresponding to the cold discomfort, temperatures are spread between 31.5°C and 35°C, with torso temperature in the lower part of the range and head temperature towards the upper end of the range. The left and right elbow are grouped together just above the middle of the interval (33.9°C), while the remaining patches are grouped

Table 6: Correlation matrix for all body parts.

	LH	LE	LS	RH	RE	RS	Head	Torso
LH	1.00	0.68	0.64	0.92	0.65	0.63	0.68	0.63
LE	0.68	1.00	0.78	0.66	0.71	0.74	0.67	0.68
LS	0.64	0.78	1.00	0.64	0.58	0.93	0.85	0.90
RH	0.92	0.66	0.64	1.00	0.59	0.62	0.61	0.63
RE	0.65	0.71	0.58	0.59	1.00	0.59	0.57	0.54
RS	0.63	0.74	0.93	0.62	0.59	1.00	0.80	0.90
Head	0.68	0.67	0.85	0.61	0.57	0.80	1.00	0.87
Torso	0.63	0.68	0.90	0.63	0.54	0.90	0.87	1.00

Table 7: PCA output for 1 component.

Body Part	PC1	h^2	u^2
LS	0.94	0.89	0.11
Torso	0.92	0.85	0.15
Head	0.92	0.84	0.16
LE	0.85	0.73	0.27
LH	0.81	0.65	0.35

around 32.8°C. On the other side of the graphic, corresponding to warm discomfort, it can be observed that most temperatures are in a much narrower range between 34.9°C and 35.5°C, with head temperature the only one outside this range, at around 37.0°C.

Based on this observation, a new set of derived measurements was proposed. Using torso temperature as the clothing reference measurement, because it had the most stable response, we computed the temperature differences between this reference and all other patch temperatures. Also, as concluded in the previous section and as shown in Figure 7a, corresponding body parts from left and right arm tend to group together, and thus, we only need to use one of them (we used the left arm). The resulting differences are plotted in Figure 7b.

The figures show that temperature differences decrease with the increase in TCV level. A possible explanation of the observed behavior is related to human body thermoregulation and heat transfer. When heat transfer between skin and environment (or clothes) was at minimum (cold discomfort) the clothing temperature tended to reflect the environment temperature. In contrast, when heat transfer was at maximum (warm discomfort), the clothing temperature tended to reflect the skin temperature. Thus, a low heat transfer corresponds to a big temperature difference between patches, while a high heat transfer corresponds to a small temperature difference. As in the case of base features, we analyzed the impact of gender, TCV level and their interaction on the temperature differences using Repeated Measure Factorial ANOVA Test. Results are presented in Table 8.

Table 8 shows that the interaction between gender and TCV level was not significant for all derived measures. Also, ignoring TCV level, the gender of the subject did not influence the temperature differences (p-value > .05). However, ignoring gender, the TCV level was significant for most temperature differences (except Shoulder-Torso and Hand-Torso). This result is useful because it suggests the use in thermal comfort modeling of the derived measures enabled by our combined sensors.

Finally, we examined a second derived set of measurements inspired by multiple thermal comfort studies

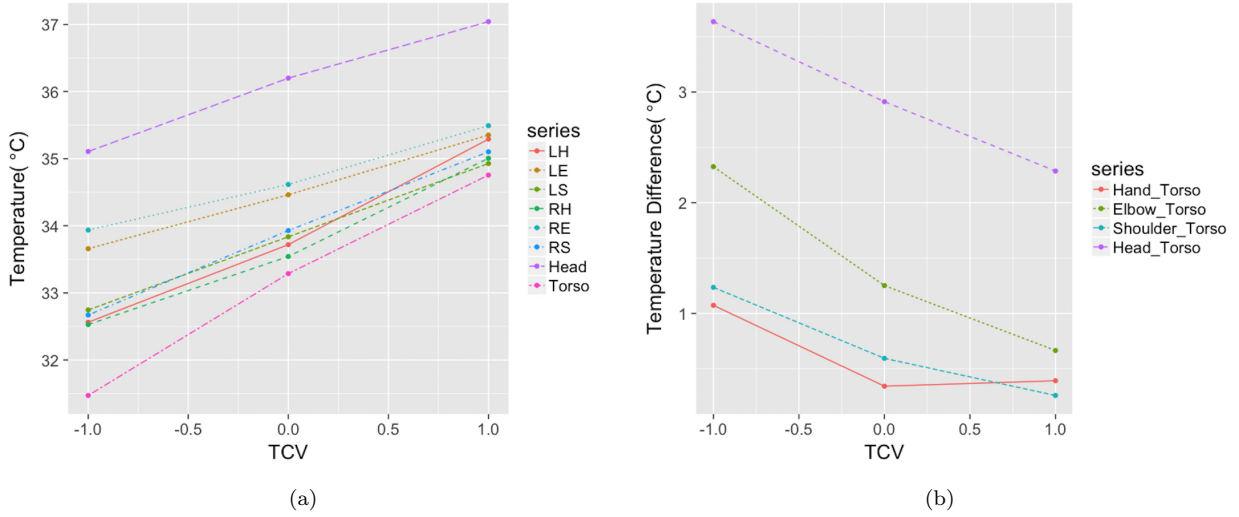


Figure 7: Average patch temperature (a) and temperature differences (b) for selected TCV levels.

Table 8: Repeated measures Factorial ANOVA test for temperature differences.

TCV Levels	Feature	Gender		TCV		Gender:TCV		Assumptions	
		F(1,10/16)	p-value	F(1,10/16)	p-value	F(1,10/16)	p-value	Normality ^a	HOV ^b
-1 and 0	Hand-Torso	0.145	0.716	13.760	0.009	2.233	0.185	✓	✓
	Elbow-Torso	2.414	0.171	9.719	0.020	0.245	0.638	✓	✓
	Shoulder-Torso	0.000	0.992	4.191	0.086	0.462	0.522	X	✓
	Head-Torso	0.140	0.721	15.678	0.007	1.439	0.275	✓	✓
0 and +1	Hand-Torso	0.000	0.997	0.380	0.551	3.049	0.111	✓	X
	Elbow-Torso	1.950	0.193	23.918	0.0006	2.106	0.069	✓	✓
	Shoulder-Torso	0.123	0.733	21.483	0.0009	1.031	0.333	✓	✓
	Head-Torso	0.000	0.995	14.364	0.003	0.905	0.363	✓	✓

^a Normality tested using Shapiro-Wilk Test

^b Homogeneity of variance(HOV) tested using Levene's Test

[24, 26, 27], based on which temperature varies significantly in body areas with high density of blood vessels (such as face and hands), and multiple key points were defined in those body areas to analyze the thermal comfort. This variance in temperature is of high interest for us, since our patch definition matches the areas of interest for these studies. Furthermore, our system offer access to dense temperature points measurements, in contrast with the sparse points used in the previous studies. These results are presented in Figure 8.

As the results show, the patch associated with the face area returns consistent results with TCV levels. When subjects felt cold discomfort, there was a high variance in patch temperatures (variance=1.1°C), while when they felt warm discomfort, the variance in temperature was lower (variance=0.55°C). Similar results were observed at the elbow, shoulder and torso level. However, both hands did not return a consistent variance trend with the TCV levels. We finished the variance analysis with a Repeated Measurements Factorial ANOVA test, as we did for all other measurements (derived or base). The results are shown in Table 9.

Based on these results, we can confirm that the temperature variance for head and torso was significantly different for the three TCV levels. But, all other body parts failed at least one assumption test, the normality test or the homogeneity of variance test, making the ANOVA test inapplicable for those. The main reason for

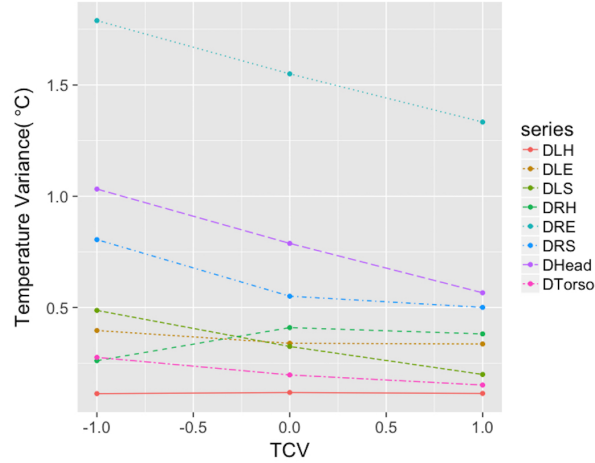


Figure 8: Average patch temperature variance for selected TCV levels.

failing the normality or homogeneity of variance test was the presence of significant noise in the measurements. We discuss this in more detail in Section 3.4.

3.4 Challenges in data collection

While our proposed non-invasive technology is a contact-less way of automatically measuring the occupant’s thermal comfort, there were multiple challenges with this approach. First, the sensors used to build the sensing platform have their own limitations. Second, the automatic procedure to extract thermal profiles of different body parts acts in a complex and continuously changing environment, where the subject is often moving (see Figure 9 for example images).

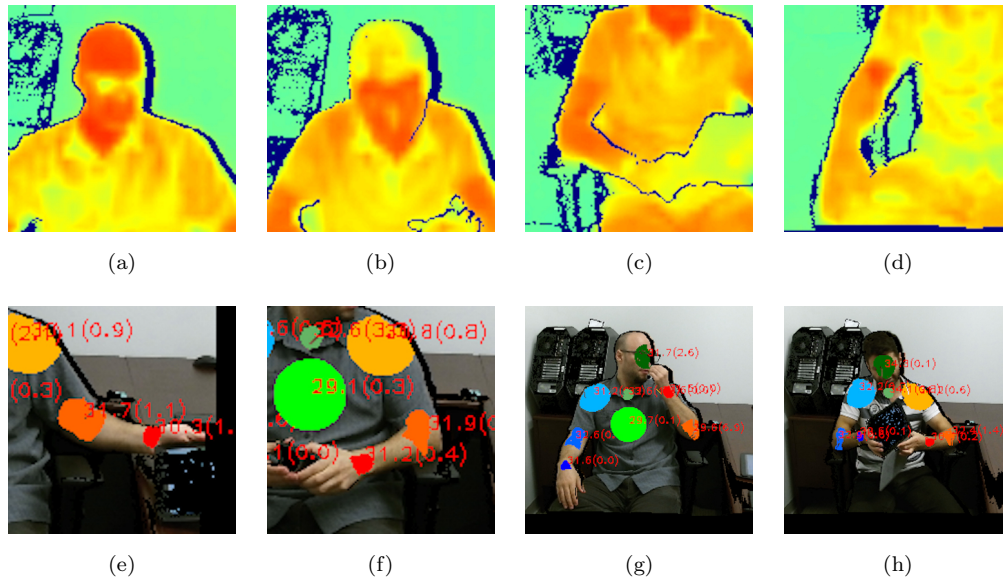


Figure 9: Sources of noise in data collection: (a)-(b) with-without sunglasses, (c)-(d) with-without hand watch, (e)-(f) inside-outside elbow and hand patch, (g)-(h) shoulder-torso occlusion.

Table 9: Repeated measures Factorial ANOVA test for patch variance measure.

TCV Levels	Body Part	Gender		TCV		Gender:TCV		Assumptions	
		F(1,10/16)	p-value	F(1,10/16)	p-value	F(1,10/16)	p-value	Normality ^a	HOV ^b
-1 and 0	Hand	0.448	0.528	1.456	0.273	0.286	0.612	✓	✓
	Elbow	0.618	0.462	0.568	0.479	0.080	0.787	X	✓
	Shoulder	3.719	0.102	12.463	0.012	2.427	0.170	X	✓
	Torso	2.855	0.142	14.237	0.009	0.373	0.563	✓	✓
	Head	0.051	0.828	6.707	0.041	0.041	0.846	✓	✓
0 and +1	Hand	3.976	0.081	6.095	0.038	1.114	0.322	X	✓
	Elbow	0.045	0.838	0.653	0.442	0.753	0.411	✓	✓
	Shoulder	6.705	0.041	7.786	0.031	2.257	0.183	✓	X
	Torso	8.664	0.018	8.161	0.021	1.422	0.267	✓	X
	Head	3.846	0.078	36.574	0.0001	2.076	0.180	✓	✓

^a Normality tested using Shapiro-Wilk Test

^b Homogeneity of variance(HOV) tested using Levene's Test

With respect to the sensor limitations, the main problems were with the thermographic camera. This had a significantly lower image resolution (80 by 60 pixels) than more expensive cameras and the temperature value accuracy for individual pixels was within 1°C, which is slightly lower than other technologies used in the literature to measure skin temperature. However, the advantage of this technology was that it allowed us to easily measure in a single frame the temperature over an area, beyond just a single point, such that noisy temperature measurements were discarded. So, the resulting average temperature measurement over an area improved the overall temperature accuracy. Moreover, the thermal images were collected at nine frames per second, while only one measurement for each minute was necessary for the thermal comfort analysis. Now, given that skin temperature varies smoothly in time, this allowed us to use all 540 frames (60 * 9) to fit a polynomial function to better approximate the instantaneous temperature at preferred time, associated with subject's feedback. Finally, the image low resolution impacted the level of detail on surface temperature (see Figure 9a-9d), which limited the accuracy of the temperature variance of each patch. However, consumer grade thermographic cameras are new to the market and higher resolution sensors will likely be available in the future.

The second challenge mentioned above had to do with the automatic procedure for extracting meaningful data for thermal comfort modeling. This procedure was affected by the human subjects variety in appearances (see Figure 9a-9d), their continuous motion (see Figure 9e-9f) and occlusions (Figure 9g-9h). The last two had the most impact on the accuracy of detecting body parts, which is of importance for the average patch temperature computation. Furthermore, the variety in appearances had a significant impact on both the average and the variance of the patch temperature. For example, subjects' accessories such as watches (Figure 9c), bracelets, or eye glasses (Figure 9a) overlapped with body parts of interest and they become part of the detected patch, influencing the average temperature and its variance. These types of limitations are to be expected in any non-invasive at-a-distance sensor measurement with low cost consumer-grade sensors.

To handle these challenges, a first corrective action was to impose a smoothness constraint on the patch temperature, such that big temperature jumps were discarded as noisy outliers. This is a fair assumption given that the temperature of each patch was computed at 10 frames per second. This measure helped to reduce the noise from detection precision and temporary occlusions. A second corrective measure was to extract the temperature information for each body part using an automatically computed patch, as defined in Section 2.2.2. This ensured a consistent body part detection at the patch level, and it helped to reduce the noise due to accessories that overlapped with target areas.

4 Conclusion

In this paper, we proposed a non-invasive and contact-less technique to model human thermal comfort in transient conditions using a novel fused-sensor visual sensing system. This consisted of three cameras (color, depth and thermal) to generate an augmented world representation, which we called RGB-DT. Using this representation, the system automatically identifies, tracks and models thermal comfort of the occupants of an office space in real time (9 fps). The combined sensor was used to extract skin and clothing temperature from different body locations that would typically be visible on a subject within a standard office setting (e.g. arms, head, and chest).

Thermal profiles for each body part were extracted from the RGB-DT model. This was defined as the average skin or clothing temperature of an area (patch) around the center point of the body part. The patch based approach, as opposed to the single point, helped reduce noise and improve stability of the generated thermal profiles. However, in situations where the subject wore accessories (such as eye glasses or watch), it was more difficult to eliminate the noise introduced, especially if the central point of the body part was located on the accessory surface.

The proposed system and algorithms were validated in a real office setting, using 30 human subjects. Although all subjects were exposed to the same temperatures, their reported comfort was significantly different. For example, only 8 subjects experienced 3 comfort levels, while 16 of them experienced just 2 of them (-1 and 0, or 0 and +1), and 6 subjects experienced only one. These findings support the recent research in the literature that argues against the feasibility of currently used thermal model to keep everyone comfortable while using only environment related measurement and ignoring the occupants' real thermal needs.

Our data analysis of skin and clothing temperature showed that these two measurements, taken at different body locations, were of high importance for the thermal comfort level. To the best of our knowledge, this was the first work that used skin and clothing temperature to model thermal comfort. We acknowledge that the clothing insulation was constant during our experiment and different clothing insulation will affect the clothing temperature readings. For this reason, it would be useful to conduct multiple experiments in the future to understand if a single thermal model based on skin and clothing temperatures can be used for mixed clothing insulation levels. In this case, the approach proposed here could be used to build multiple parallel models for different groups of insulation. However, automated discovery of such clothing groups and such a multiple-model study is beyond the scope of this paper. Also, an investigation of the BMI impact on the thermal comfort was not considered, while it was showed in [23] that BMI has an important role in thermal sensation assessment. We plan to address these topics in a later experiment.

We also proposed a new set of derived measurements to be used together with the base skin and clothing temperature to model thermal comfort. These were inspired from thermoregulation effects on skin temperature and evidence extracted from collected data. We found that the temperature differences between body parts were relevant for the three thermal comfort levels. There was a high temperature difference between body parts, when subjects were feeling cold discomfort, while these differences were much smaller for warm discomfort. Also, the temperature variance of each patch was an indicator of thermal comfort, with a high variance when feeling cold discomfort, and a low variance for warm discomfort.

Finally, results showed that thermal comfort can be derived from observing only one arm, because there was a high correlation between the thermal profiles of the left and right arms of all subjects throughout the tests. This was an important observation, since in an office setup, a fixed-location sensor will only see some parts of an occupant.

This work is a first step towards a new generation of intelligent heating and cooling systems that avoid any contact with occupants. These systems will continuously monitor the environment and act in response to a real thermal need of the occupants. Further research is required to evaluate the feasibility of such a system across different types of environments (residential, commercial and industrial) and different occupants' activities (sports, driving and sleeping).

References

- [1] Commercial buildings energy consumption survey (CBECS), <https://www.eia.gov/consumption/commercial/data/2012/>, Last Accessed: 30-May-2018 (2012).
- [2] Residential energy consumption survey (RECS), <https://www.eia.gov/consumption/residential/data/2015/>, Last Accessed: 30-May-2018 (2015).
- [3] P. O. Fanger, Thermal comfort: Analysis and applications in environmental engineering, Danish Technical Press, 1970.
URL <https://books.google.com/books?id=S0FSAAAAMAAJ>
- [4] C. Huizenga, S. Abbaszadeh, L. Zagreus, E. A. Arens, Air quality and thermal comfort in office buildings: results of a large indoor environmental quality survey, Proceedings of Healthy Buildings III (2006) 393–397.
- [5] J. V. Hoof, Forty years of fanger’s model of thermal comfort: comfort for all?, Indoor Air 18 (3) (2007) 182–201. arXiv:<https://onlinelibrary.wiley.com/doi/pdf/10.1111/j.1600-0668.2007.00516.x>, doi:10.1111/j.1600-0668.2007.00516.x.
URL <https://onlinelibrary.wiley.com/doi/abs/10.1111/j.1600-0668.2007.00516.x>
- [6] M. Fountain, G. Brager, R. de Dear, Expectations of indoor climate control, Energy and Buildings 24 (3) (1996) 179 – 182. doi:[https://doi.org/10.1016/S0378-7788\(96\)00988-7](https://doi.org/10.1016/S0378-7788(96)00988-7).
URL <http://www.sciencedirect.com/science/article/pii/S0378778896009887>
- [7] W. Liu, Z. Lian, Q. Deng, Y. Liu, Evaluation of calculation methods of mean skin temperature for use in thermal comfort study, Building and Environment 46 (2) (2011) 478 – 488. doi:<https://doi.org/10.1016/j.buildenv.2010.08.011>.
URL <http://www.sciencedirect.com/science/article/pii/S0360132310002647>
- [8] F. Jazizadeh, F. M. Marin, B. Becerik-Gerber, A thermal preference scale for personalized comfort profile identification via participatory sensing, Building and Environment 68 (2013) 140 – 149. doi:<https://doi.org/10.1016/j.buildenv.2013.06.011>.
URL <http://www.sciencedirect.com/science/article/pii/S0360132313001893>
- [9] F. Jazizadeh, A. Ghahramani, B. Becerik-Gerber, T. Kichkaylo, M. Orosz, User-led decentralized thermal comfort driven hvac operations for improved efficiency in office buildings, Energy and Buildings 70 (2014) 398 – 410. doi:<https://doi.org/10.1016/j.enbuild.2013.11.066>.
URL <http://www.sciencedirect.com/science/article/pii/S0378778813007731>
- [10] B. Balaji, H. Teraoka, R. Gupta, Y. Agarwal, Zonpac: Zonal power estimation and control via hvac metering and occupant feedback, in: Proceedings of the 5th ACM Workshop on Embedded Systems For Energy-Efficient Buildings, BuildSys’13, ACM, New York, NY, USA, 2013, pp. 18:1–18:8. doi:10.1145/2528282.2528304.
URL <http://doi.acm.org/10.1145/2528282.2528304>
- [11] S. Karjalainen, O. Koistinen, User problems with individual temperature control in offices, Building and Environment 42 (8) (2007) 2880 – 2887. doi:<https://doi.org/10.1016/j.buildenv.2006.10.031>.
URL <http://www.sciencedirect.com/science/article/pii/S0360132306003349>
- [12] W. Pasut, H. Zhang, E. Arens, Y. Zhai, Energy-efficient comfort with a heated/cooled chair: Results from human subject tests, Building and Environment 84 (2015) 10 – 21. doi:<https://doi.org/10.1016/j.buildenv.2014.10.026>.
URL <http://www.sciencedirect.com/science/article/pii/S0360132314003473>
- [13] H. Zhang, E. Arens, M. Taub, D. Dickerhoff, F. Bauman, M. Fountain, W. Pasut, D. Fannon, Y. Zhai, M. Pigman, Using footwarmers in offices for thermal comfort and energy savings, Energy and Buildings 104 (2015) 233 – 243. doi:<https://doi.org/10.1016/j.enbuild.2015.06.086>.
URL <http://www.sciencedirect.com/science/article/pii/S0378778815301067>

- [14] S. Liu, L. Yin, W. K. Ho, K. V. Ling, S. Schiavon, A tracking cooling fan using geofence and camera-based indoor localization, *Building and Environment* 114 (2017) 36 – 44. doi:<https://doi.org/10.1016/j.buildenv.2016.11.047>.
URL <http://www.sciencedirect.com/science/article/pii/S0360132316304784>
- [15] R. F. Rupp, N. G. Vasquez, R. Lamberts, A review of human thermal comfort in the built environment, *Energy and Buildings* 105 (2015) 178 – 205. doi:<https://doi.org/10.1016/j.enbuild.2015.07.047>.
URL <http://www.sciencedirect.com/science/article/pii/S0378778815301638>
- [16] A. A. Farhan, K. Pattipati, B. Wang, P. B. Luh, Predicting individual thermal comfort using machine learning algorithms, in: 2015 IEEE International Conference on Automation Science and Engineering (CASE), 2015, pp. 708–713. doi:10.1109/CoASE.2015.7294164.
- [17] T. Chaudhuri, Y. C. S. andd Hua Li, L. Xie, Machine learning based prediction of thermal comfort in buildings of equatorial singapore, in: 2017 IEEE International Conference on Smart Grid and Smart Cities (ICSGSC), 2017, pp. 72–77. doi:10.1109/ICSGSC.2017.8038552.
- [18] W. Liu, Z. Lian, Y. Liu, Heart rate variability at different thermal comfort levels, *European Journal of Applied Physiology* 103 (3) (2008) 361–366. doi:10.1007/s00421-008-0718-6.
URL <https://doi.org/10.1007/s00421-008-0718-6>
- [19] J.-H. Choi, V. Loftness, Investigation of human body skin temperatures as a bio-signal to indicate overall thermal sensations, *Building and Environment* 58 (2012) 258 – 269. doi:<https://doi.org/10.1016/j.buildenv.2012.07.003>.
- [20] Q. Jin, X. Li, L. Duanmu, H. Shu, Y. Sun, Q. Ding, Predictive model of local and overall thermal sensations for non-uniform environments, *Building and Environment* 51 (2012) 330 – 344. doi:<https://doi.org/10.1016/j.buildenv.2011.12.005>.
URL <http://www.sciencedirect.com/science/article/pii/S0360132311004215>
- [21] C. Dai, H. Zhang, E. Arens, Z. Lian, Machine learning approaches to predict thermal demands using skin temperatures: Steady-state conditions, *Building and Environment* 114 (2017) 1 – 10. doi:<https://doi.org/10.1016/j.buildenv.2016.12.005>.
URL <http://www.sciencedirect.com/science/article/pii/S036013231630484X>
- [22] T. Chaudhuri, D. Zhai, Y. C. Soh, H. Li, L. Xie, Thermal comfort prediction using normalized skin temperature in a uniform built environment, *Energy and Buildings* 159 (2018) 426 – 440. doi:<https://doi.org/10.1016/j.enbuild.2017.10.098>.
URL <http://www.sciencedirect.com/science/article/pii/S0378778817327354>
- [23] J.-H. Choi, D. Yeom, Study of data-driven thermal sensation prediction model as a function of local body skin temperatures in a built environment, *Building and Environment* 121 (2017) 130 – 147. doi:<https://doi.org/10.1016/j.buildenv.2017.05.004>.
URL <http://www.sciencedirect.com/science/article/pii/S0360132317301841>
- [24] A. Ghahramani, G. Castro, B. Becerik-Gerber, X. Yu, Infrared thermography of human face for monitoring thermoregulation performance and estimating personal thermal comfort, *Building and Environment* 109 (2016) 1 – 11. doi:<https://doi.org/10.1016/j.buildenv.2016.09.005>.
URL <http://www.sciencedirect.com/science/article/pii/S0360132316303456>
- [25] M. Burzo, C. Wicaksono, M. Abouelenien, V. Perez-Rosas, R. Mihalcea, Y. Tao, Multimodal sensing of thermal discomfort for adaptive energy saving in buildings, *iiSBE NET ZERO BUILT ENVIRONMENT* (2014) 344.
- [26] B. Pavlin, G. Pernigotto, F. Cappelletti, P. Bison, R. Vidoni, A. Gasparella, Real-time monitoring of occupants' thermal comfort through infrared imaging: A preliminary study, *Buildings* 7 (1). doi:10.3390/buildings7010010.
URL <http://www.mdpi.com/2075-5309/7/1/10>

- [27] J. Ranjan, J. Scott, Thermalsense: Determining dynamic thermal comfort preferences using thermographic imaging, in: Proceedings of the 2016 ACM International Joint Conference on Pervasive and Ubiquitous Computing, UbiComp '16, ACM, New York, NY, USA, 2016, pp. 1212–1222. doi:10.1145/2971648.2971659.
URL <http://doi.acm.org/10.1145/2971648.2971659>
- [28] ASHRAE, ANSI/ASHRAE Standard 55: Thermal Environmental Conditions for Human Occupancy, American Society of Heating, Refrigerating and Air Conditioning Engineers, Atlanta, Georgia, 2013.
- [29] Center for Building Performance and Diagnostics, GSA workplace 2020 project technical report to the U.S. General Services Administration (2008).
- [30] T. Bedford, The warmth factor in comfort at work: a physiological study of heating and ventilation, H.M. Stationery Off., London, Great Britain, 1936.